06.1;04.1

Synthesis of aluminum-magnesium spinel nanopowder in an electric arc plasmatron

© V.V. Lisenkov[1,2], V.V. Osipov[1], A.V. Podkin[1], I.N. Tikhonov[2]

[1] Institute of Electrophysics, Ural Branch, Russian Academy of Sciences, Yekaterinburg, Russia
[2] Ural Federal University after the first President of Russia B.N. Yeltsin, Yekaterinburg, Russia
E-mail: lisenkov@iep.uran.ru, v.v.lisenkov@urfu.ru

Received December 14, 2023
Revised March 1, 2024
Accepted March 10, 2024

The paper presents the results of an experiment on the synthesis of aluminum-magnesium spinel nanoparticles using an electric arc plasmatron. Metal powders of aluminum and magnesium were used as raw materials. The metal powder particles burned almost completely, ensuring the appearance of the desired oxides in the gas phase, which is a necessary condition for the synthesis of nanoparticles. As a result, a weakly agglomerated nanopowder of the composition Al−Mg spinel (~ 52 mass%), Al_2O_3 (~ 32 mass%) and MgO (~ 16 mass%) in the cubic phase was obtained, having a narrow size distribution (17 nm at half maximum) and a particle diameter of 10 nm at maximum of distribution functions.

Keywords: synthesis of nanoparticles, electric arc plasmatron.

DOI: 10.61011/TPL.2024.06.58482.19846

Refinement of techniques for nanopowder synthesis is a relevant task. Plasma methods occupy their rightful place among various kinds of physical and chemical methods. A plasmatron is the most widely used instrument for plasma generation. However, it is difficult to generate plasma with a boiling temperature of refractory oxides. This is the reason why various easily decomposable chemical compounds containing the needed metal (or metal with oxygen) are used for their production. However, both the initial reagents and certain reaction products are hazardous and even toxic (see, e.g., [1,2], where the synthesis of titanium and zirconium nanopowders with the use of $TiCl_4$ and $ZrCl_4$, respectively, was reported).

A reaction of metal combustion, which is initiated and sustained by a plasmatron and also allows one to produce oxide molecules in the gas phase with a capacity to condense into nanoparticles, is a viable alternative in this context. This process has been examined earlier in [3,4] (for aluminum and magnesium oxides) and in several studies cited in review [5] (for other oxides). However, the synthesis of an Al−Mg spinel nanopowder from metal powders burning with an exothermic effect, which facilitates the production of a mixture of needed oxides in the has phase, has not been reported yet. The exothermic effect of burning of hydrocarbons initiated by a plasmatron has been used in [6] to synthesize a tungsten carbide nanopowder. At the same time, an Al−Mg spinel nanopowder has been synthesized successfully in [7,8] by laser evaporation of a mechanical mixture of Al_2O_3 and MgO powders. The technology of spinel nanopowder synthesis used in the indicated studies is significantly less complex than chemical techniques employed traditionally for spinel synthesis, such as self-propagating high-temperature synthesis (see, e.g., [9,10]), high-temperature synthesis with a plasmatron [11], and the sol–gel method (see, e.g., [12]). In addition, the mentioned chemical processes do not allow one to produce nanopowders of a sufficiently high quality (or are completely unsuitable for nanopowder production), and some of them involve the use of hazardous chemical compounds.

Owing to its high surface energy, an Al−Mg spinel nanopowder offers good prospects for synthesis of transparent ceramic elements. It is known [13] that Al−Mg spinel ceramics are suitable for fabrication of fairings for aviation, rocket, and space equipment. Such materials are used to produce lenses, protective windows, and body protectors.

The aim of the present study is to examine the possibility of synthesis of an Al−Mg spinel nanopowder from a mixture of Al and Mg powders with the use of an electric-arc plasmatron.

A plasmatron of a proprietary design with aluminum electrodes, which helped avoid the contamination of nanopowders with foreign materials, was used. The diagram of the setup is shown in Fig. 1. The metal powder used was a mechanical mixture of Al particles $200-300\,\mu$m in size and Mg−Al alloy (Mg:Al = 9:1) particles with a size of $100-200\,\mu$m in a mass proportion of 2.25:1. This proportion was set for the reason that it provided the best results in the conditions of experiments mentioned above. The indicated powder was fed into a plasma jet together with air, where oxides in the gas phase, which then condensed into nanoparticles, formed under the combined thermal influence of plasma and the oxidation reaction. Hot air with nanoparticles entered a cyclone that separated unburnt particles. Having passed through the cyclone and a cooling system, a suspension of nanoparticles in gas reached the fabric filter (similar to the one installed in the setup used in [7]) for nanoparticle collection. Air was then released into the atmosphere through an additional filter. The plasmatron

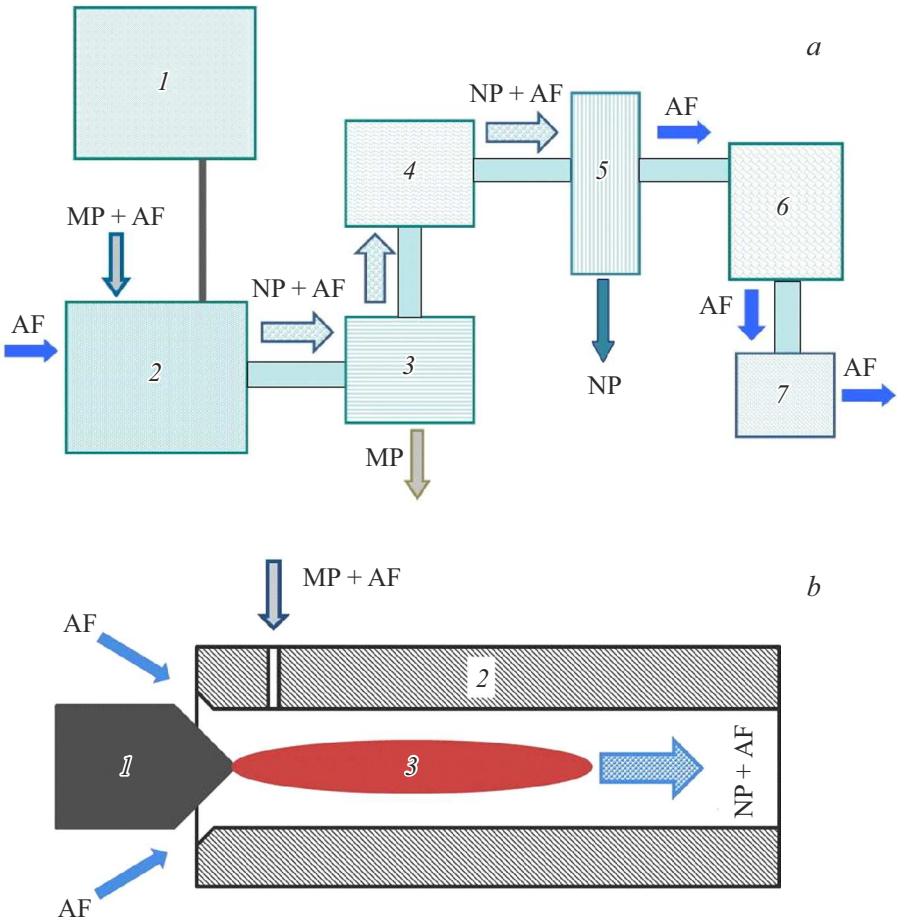

Figure 1. Diagram of the experimental setup. AF — Air flow, MP — metal particles, NP — nanoparticles. *a* — Overall diagram: *1* — power supply, *2* — electrode assembly (see panel *b*), *3* — cyclone for separation of unburnt metal particles, *4* — air flow cooling system, *5* — fabric filter for nanoparticle collection, *6* — evacuation pump, and *7* — filter for final air cleaning. *b* — Diagram of the electrode assembly of the plasmatron: *1* — cathode, *2* — anode with an aperture for supply of metal particles, and *3* — arc discharge plasma.

was supplied by a standard Svarog Real Cut 90 (L205) source for plasma cutting with a capacity to maintain the specified DC current. The dynamics of plasmatron voltage (see Fig. 2) is indicative of a turbulent nature of gas flow and the corresponding arcing regime. This regime is known and has been characterized in review [14]. The average arcing power at an operating current of 28 and 37 A was 2140 and 2360 W, respectively. It was calculated as a time integral of the product of the corresponding current and instantaneous voltage values (see Fig. 2). The air flow rate in the plasmatron was approximately 24 l/s, which corresponded to a flow velocity around 100 m/s in the arc region.

Figure 3 presents the microphotographic image of the obtained nanopowder (*a*) and its distribution function (*b*) and diffraction pattern (*c*), which reveals the phase composition. The microphotographic image in Fig. 3, *a* and other images used for plotting the size distribution function were made with a transmission electron microscope by laboratory personnel at the Common Use Center of the Institute of New Materials and Technologies (Ural Federal University). This image makes it evident that the nanopowder is weakly

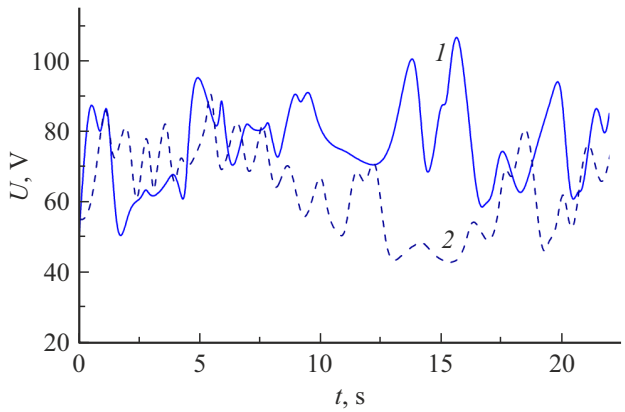

Figure 2. Dynamics of plasmatron voltage at a current of 28 (*1*) and 37 A (*2*).

agglomerated and its particles have a round shape, which is indicative of their condensation from a gas phase into a liquid one with subsequent crystallization in the course of cooling in air flow. To plot the size distribution function

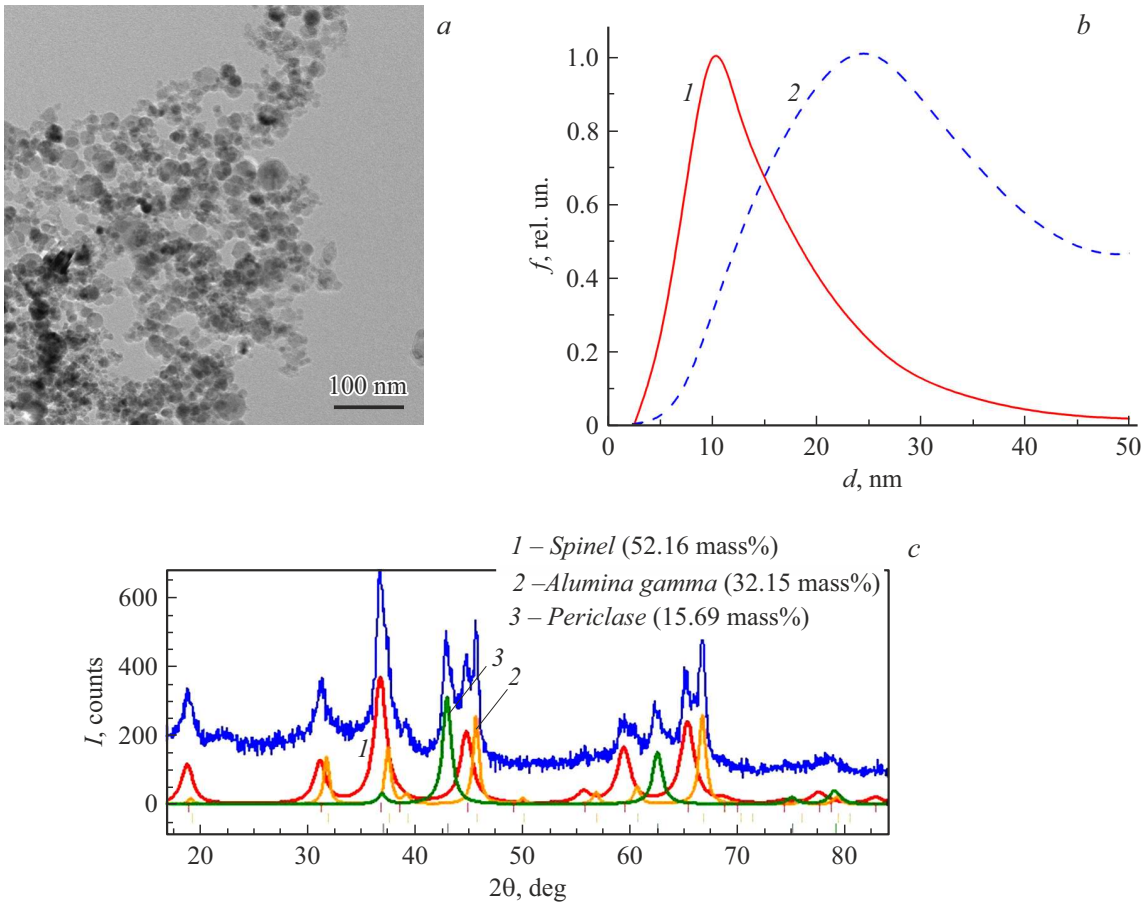

Figure 3. Properties of the obtained nanopowder. *a* — Microphotographic image of nanoparticles. *b* — Diameter distribution functions of nanoparticles. Curves *1* and *2* represent number and mass distributions of nanoparticles, respectively. The integral under curve *1* is proportional to the overall number of nanoparticles, while the integral under curve *2* is proportional to the overall mass of nanoparticles. *c* — Diffraction pattern of the nanopowder.

of nanoparticles, diameters were measured for a total of approximately 10 000 particles in a series of electron-microscopic images. This allowed us to obtain a fairly smooth distribution. Particles with a size around 10 nm are dominant in the nanopowder (curve *1* in Fig. 3. *b*), and the number distribution is rather narrow (17 nm at half height). These parameters are somewhat lower than in [7]. However, the greatest mass fraction in the nanopowder belongs to particles with a size of approximately 25 nm (curve *2*), and the mass distribution is broader: 32 nm at half height (a mass distribution was not plotted in [7]). The obtained data suggest that the process of condensation in our experiment is accompanied by coalescence of nanoparticles in a liquid state; i.e., the processes are generally the same as those observed in nanopowder synthesis in laser plasma [5,6].

The authors of [8] determined the phase composition of nanoparticles in accordance with the procedure outlined in [7,8]. Figure. 3, *c* presents the diffraction pattern of the synthesized nanopowder. It was obtained using a D8 DISCOVER diffractometer with copper radiation ($CuK_{\alpha 1,2} = 1.542$ Å) and a graphite monochromator for the diffracted beam. Processing was performed in TOPAS 3. According to the obtained data, the nanopowder synthesized from a mixture of metal aluminum and magnesium powders contained Al–Mg spinel (~ 52 mass%), Al_2O_3 (~ 32 mass%), and MgO (~ 16 mass%) in the cubic phase. In view of the accuracy of the method used, it appears correct to round the results presented in Fig. 3, *c* to the nearest integer percent values. A similar pattern was observed in [7], where a weakly agglomerated nanopowder of the following composition was synthesized by laser evaporation of a mechanical mixture of oxide powders: Al–Mg spinel (67.5 mass%), Al_2O_3 (24.8 mass%), MgO (4.5 mass%), and Fe_3O_4 (3.2 mass%) (iron oxide was added to the evaporated mixture in [7]). This is also indicative of similarity between the mechanisms of nanopowder synthesis in laser flare plasma and in the conditions of our experiment.

The presence of aluminum and magnesium oxides (as impurities) in nanopowders synthesized both in the present study and in [7,8] still remains unexplained. It would seem that regardless of the method of its production, vapor consisting of a mixture of aluminum and magnesium oxides should condense into liquid nanoparticles consisting of the same oxides, and Al–Mg spinel should form upon

crystallization of these nanoparticles. However, this process is only partial: the mass fraction of nanoparticles in the spinel phase is ~ 52 mass% in our experiment and 67.5 mass% in [7]. Two probable causes of partial formation of Al and Mg oxides in the nanopowder studied here may be identified. The first one is that a certain fraction of oxide vapors manages to condense in the immediate vicinity of burning metal particles of the charge stock before turbulent mixing of oxide vapors in air flow occurs. The second cause factor is related to the statistics of formation of $MgAl_2O_4$, Al_2O_3, and MgO critical nuclei, which makes condensation into these three compounds in the obtained proportions energetically favorable. This inference is supported by the qualitative agreement between our data and the results reported in [7], where oxides were mixed almost immediately upon evaporation. However, other cause factors related to the kinetics of condensation of a vapor mixture of Al and Mg oxides and the coalescence of nanoparticles in the liquid phase, which still remains uninvestigated (at least in the conditions of our experiment and the experiments performed in [7,8]), may also be involved. A thorough examination of the indicated factors and a search for the ways to increase the fraction of spinel in a nanopowder will be performed in our future studies.

We note in conclusion that, first, the ratio of free Al and Mg oxides in the nanopowder is virtually the same as the one needed for spinel synthesis from powder mixtures. Therefore, the obtained powder allows one to sinter ceramic samples consisting entirely of spinel. Second, the method used in the present study does not involve complex procedures and hazardous reagents (in contrast to chemical methods) and does not require costly laser equipment (in contrast to [7,8]). In addition, the use of aluminum electrodes in the plasmatron helps avoid the contamination of nanopowders with foreign materials. All the above factors and the relative ease of implementation make the proposed method promising for industrial application (with regard not only to Al–Mg spinel, but also to other oxide nanopowders, including those with a complex composition) after a certain refinement.

Acknowledgments

The authors wish to thank their colleagues at the Pulsed Processes Laboratory (Institute of Electrophysics, Ural Branch, Russian Academy of Sciences) and the Common Use Center of the Institute of New Materials and Technologies (Ural Federal University) for performing X-ray diffraction analysis and electron-microscopic analysis, respectively, of the obtained nanopowder.

Conflict of interest

The authors declare that they have no conflict of interest.

References

[1] E.V. Kartaev, V.P. Lukashov, S.P. Vashenko, S.M. Aulchenko, O.B. Kovalev, D.V. Sergachev, Int. J. Chem. Reactor Eng., **12**, 1 (2014). DOI: 10.1515/ijcre-2014-0001
[2] A.V. Samokhin, M.A. Sinayskiy, N.V. Alexeev, R.N. Rizakhanov, Yu.V. Tsvetkov, I.S. Litvinova, A.A. Barmin, Inorg. Mater.: Appl. Res., **6** (5), 528 (2015).
[3] G.P. Vissokov, K.D. Manolova, L.B. Brakalov, J. Mater. Sci., **16**, 1716 (1981). DOI: 10.1007/PL00020606
[4] E.I. Gusachenko, L.N. Stesik, V.P. Fursov, V.I. Shevtsov, Combust. Explos. Shock Waves, **10** (5), 588 (1974). DOI: 10.1007/BF01463970.
[5] A.N. Zolotko, Y.I. Vovchuk, N.I. Poletayev, A.V. Florko, I.S. Al'tman, Combust. Explos. Shock Waves, **32** (3), 262 (1996). DOI: 10.1007/BF01998454.
[6] Yu.V. Tsvetkov, A.V. Nikolaev, A.V. Samokhin, Avtom. Svarka, Nos. 10–11, 112 (2013) (in Russian).
[7] V.V. Osipov, V.I. Solomonov, V.V. Platonov, E.V. Tikhonov, A.I. Medvedev, Appl. Phys. A, **125**, 48 (2019). DOI: 10.1007/s00339-018-2341-7
[8] I.V. Beketov, A.I. Medvedev, O.M. Samatov, A.V. Spirina, K.I. Shabanova, J. Alloys Compd., **586**, S472 (2014). DOI: 10.1016/j.jallcom.2013.02.070
[9] V. Singha, R.P.S. Chakradhar, J.L. Rao, D.K. Kim, J. Solid State Chem., **180**, 2067 (2007). DOI: 10.1016/j.jssc.2007.04.030
[10] N.I. Radishevskaya, A.Yu. Nazarova, O.V. L'vov, N.G. Kasatskii, V.G. Salamatov, I.V. Saikov, D.Yu. Kovalev, Inorg. Mater., **56** (2), 142 (2020). DOI: 10.1134/S0020168520010112.
[11] V.V. Shekhovtsov, N.K. Skripnikova, A.B. Ulmasov, Inorg. Mater., **59** (8), 851 (2023). DOI: 10.1134/S0020168523080149.
[12] L.V. Morozova, O.L. Belousova, T.I. Panova, R.S. Shornikov, O.A. Shilova, Fiz. Khim. Stekla, **38** (6), 768 (2012) (in Russian).
[13] M.O. Senina, D.O. Lemeshev, Usp. Khim. Khim. Tekhnol., **30** (7), 101 (2016) (in Russian).
[14] M.F. Zhukov, Teplofiz. Vys. Temp., **10** (6), 1295 (1972) (in Russian).

Translated by D.Safin